Virology **301,** 109–120 (2002)
doi:10.1006/viro.2002.1551

Murine Coronavirus Spike Glycoprotein Mediates Degree of Viral Spread, Inflammation, and Virus-Induced Immunopathology in the Central Nervous System

Joanna J. Phillips,* Ming Ming Chua,* Glenn F. Rall,† and Susan R. Weiss*,[1]

*Department of Microbiology, University of Pennsylvania School of Medicine, Philadelphia, Pennsylvania 19104-6076; and †Division of Basic Science, The Fox Chase Cancer Center, 7701 Burholme Avenue, Philadelphia, Pennsylvania 19111

Received February 25, 2002; returned to author for revision April 26, 2002; accepted May 5, 2002

The mouse hepatitis virus (MHV) spike glycoprotein is a major determinant of neurovirulence. We investigated how alterations in spike affect neurovirulence using two isogenic recombinant viruses differing exclusively in spike. S_4R, containing the MHV-4 spike gene, is dramatically more neurovirulent than $S_{A59}R$, containing the MHV-A59 spike gene (J. J. Phillips, M. M. Chua, E. Lavi, and S. R. Weiss, 1999, J. Virol. 73, 7752–7760). We examined the contribution of differences in cellular tropism, viral spread, and the immune response to infection to the differential neurovirulence of S_4R and $S_{A59}R$. MHV-4 spike-mediated neurovirulence was associated with extensive viral spread in the brain in both neurons and astrocytes. Infection of primary hippocampal neuron cultures demonstrated that S_4R spread more rapidly than $S_{A59}R$ and suggested that spread may occur between cells in close physical contact. In addition, S_4R infection induced a massive influx of lymphocytes into the brain, a higher percentage of $CD8^+$ T cells, and a higher frequency of MHV-specific $CD8^+$ T cells relative $S_{A59}R$ infection. Despite this robust and viral-specific immune response to S_4R infection, infection of RAG1−/− mice suggested that immune-mediated pathology also contributes to the high neurovirulence of S_4R.

INTRODUCTION

The severity of viral infections depends on the extent of tissue destruction and cellular dysfunction mediated by a combination of direct virus infection and immune-mediated destruction. The relative contribution of these two components differs depending on a number of virus and host factors including viral tropism, rate of viral spread, and specificity of the immune response.

Infection of mice with the murine coronavirus, mouse hepatitis virus (MHV), provides a model for studying acute virus-induced neurological disease. We have previously demonstrated that the spike (S) gene is a major determinant of MHV neurovirulence. Recombinant viruses containing the spike gene of the highly neurovirulent MHV-4 strain, S_4R, exhibit a dramatically more neurovirulent phenotype (3 $\log_{10}$ decrease in intracranial LD_{50}) than isogenic recombinants containing the spike gene of the mildly neurovirulent MHV-A59 strain, $S_{A59}R$ (Phillips *et al.,* 1999). ($S_{A59}R$ and S_4R have all other genes derived from MHV- A59.) By defining the contribution of direct virus-mediated pathology and immune-mediated pathology to the differential neurovirulence of S_4R and $S_{A59}R$, we can better elucidate the mechanisms by which the MHV-4 spike confers high neurovirulence.

The MHV spike glycoprotein is required for viral entry and spread (Boyle *et al.,* 1987; Collins *et al.,* 1982; Sturman and Holmes, 1981). Expressed on the virion surface, spike is responsible for binding to the viral receptor and mediating virus–cell fusion, and subsequent to infection spike, expressed on the host cell membrane, can mediate cell–cell fusion. The spike is also vital for the immune response to infection as it is able to induce both a cell-mediated and a humoral-mediated immune response (Bergmann *et al.,* 1996; Castro and Perlman, 1995; Collins *et al.,* 1982). Thus the high neurovirulence conferred by the MHV-4 spike may be due to alterations in a number of aspects of infection including viral entry, viral spread, or the immune response to infection.

Although MHV infects many cell types in the brain, including neurons, astrocytes, and oligodendrocytes (Knobler *et al.,* 1981; Lavi *et al.,* 1984, 1988; Weiner, 1973), it has been suggested that neuronal tropism is a major determinant of MHV neurovirulence (Dubois-Dalcq *et al.,* 1982; Fleming *et al.,* 1986; Knobler *et al.,* 1981). The high neurovirulence of S_4R is associated with extensive spread of virus in the brain (Phillips *et al.,* 1999). Increased viral spread could either reflect increased infection of a particular cell-type, such as neurons, or alternatively increased infection of multiple cell types in the CNS.

In the CNS, clearance of infectious MHV requires multiple components of the immune response including $CD8^+$ and $CD4^+$ T cells and B cells. Adoptive transfer experiments in combination with depletion experiments have demonstrated that both $CD8^+$ and $CD4^+$ T cells are critical for normal viral clearance (Korner *et al.,* 1991;

[1] To whom correspondence and reprint requests should be addressed. Fax: (215) 573-4858. E-mail: weisssr@mail.med.upenn.edu.

0042-6822/02 $35.00

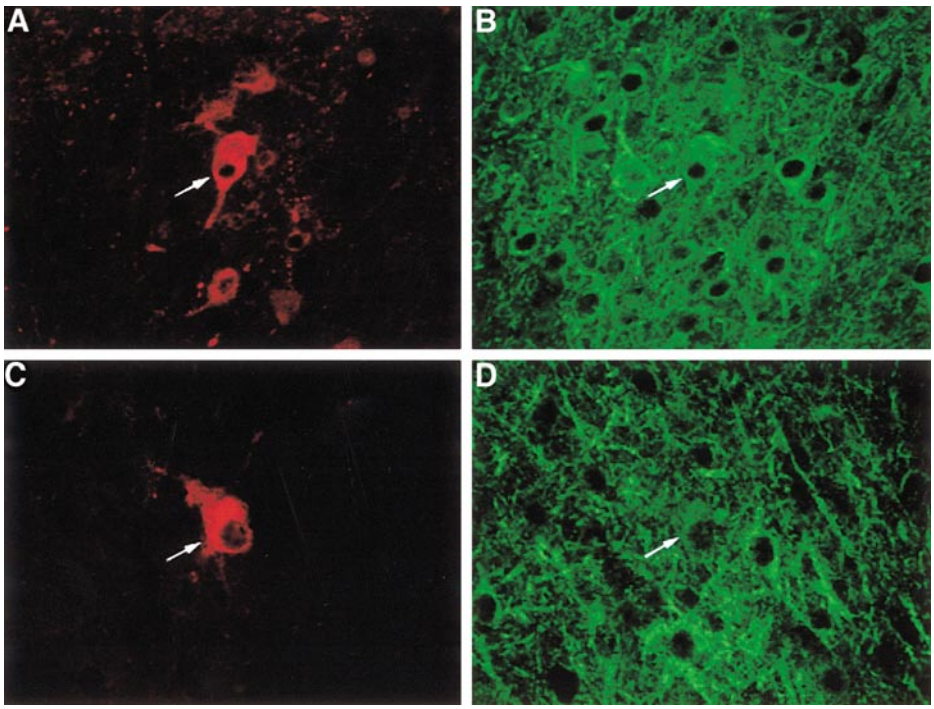

FIG. 1. Identification of S_4R- and $S_{A59}R$-infected neurons in the brain 5 days after intracranial inoculation. Representative pictures are shown of double-immunofluorescent labeling of sagittal brain sections taken from S_4R-inoculated (A and B), and $S_{A59}R$-inoculated (C and D) mice. A and C show immunofluorescent labeling of viral antigen in the basal forebrain (red). B and D show the corresponding labeling of MAP2b in neurons (green). Note MAP2b-positive cells exhibit the characteristic morphology of neurons. Arrows identify cells double-positive for viral antigen, and MAP2b in both S_4R and $S_{A59}R$ inoculated brains. Note the greater total number of viral antigen-positive cells following inoculation with S_4R. No viral antigen staining was observed in mock-infected mice, when sections were incubated in preimmune sera, or when the primary antibody was omitted (data not shown). Magnification, ×380.

Stohlman *et al.,* 1986, 1995, 1998; Sussman *et al.,* 1989; Williamson and Stohlman, 1990; Yamaguchi *et al.,* 1991). Furthermore, the peak of T lymphocyte infiltration into the CNS is coincident with falling titers of infectious virus in the CNS (Williamson *et al.,* 1991). Relative to infection with $S_{A59}R$, infection with S_4R results in a dramatic infiltration of inflammatory cells into the CNS (Phillips *et al.,* 1999). Differences in either the composition of these infiltrates or their virus-specific activity could have a profound influence on neurovirulence.

The MHV spike is a major determinant of MHV neurovirulence. To identify the critical parameters of infection mediating the differential neurovirulence of S_4R and $S_{A59}R$, we characterized the cellular tropism and composition and function of the lymphocytic response to infection with S_4R and $S_{A59}R$. Our results suggest that the high neurovirulence conferred by alterations in the MHV spike are mediated by both increased viral spread in multiple cell types in the brain and immune-mediated pathology.

RESULTS

S_4R and $S_{A59}R$ exhibit similar cellular tropism

We previously observed that at the peak of virus replication, day 5 postinfection, the more neurovirulent S_4R infects a significantly greater number of cells in the basal

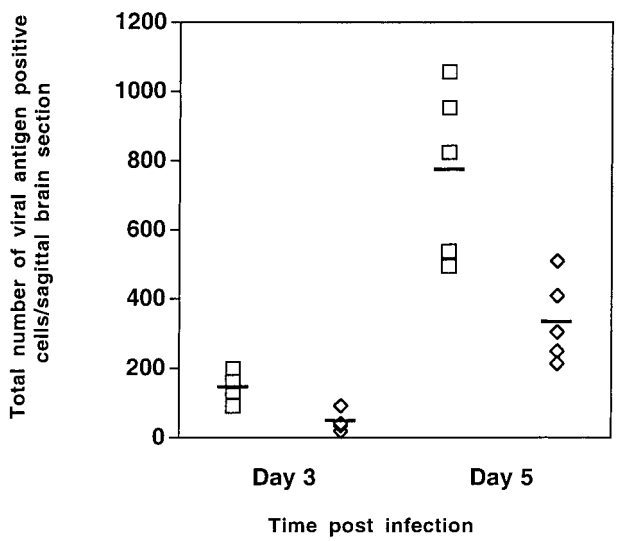

FIG. 2. Quantification of viral antigen positive cells in the brain following inoculation with S_4R and $S_{A59}R$. The total number of viral antigen-positive cells per brain section following infection with S_4R (open squares), and $S_{A59}R$ (open diamonds) was determined on days 3 and 5 postinfection. On day 5 postinfection two brain sections per mouse were examined, and the mean number of viral antigen-positive cells per sagittal section was determined ($n = 5$). For the quantification of viral antigen-positive cells on day 3 a single sagittal section was examined for each infected mouse ($n = 4$). The mean number of viral antigen-positive cells per brain section (horizontal line) following infection with S_4R was significantly greater than with $S_{A59}R$ on days 3 and 5 postinfection (two-tailed t test, $P < 0.05$, and $P < 0.001$, respectively).

TABLE 1

Identification of CNS Cells Infected by S_4R and $S_{A59}R$ on Day 5 Postinfection[a]

Virus	Animal	Section 1		Section 2	
		No. of viral antigen-positive cells	No. of cells double-positive with AP14 (%)[b]	No. of viral antigen-positive cells	No. of cells double-positive for GFAP (%)[b]
S_4R	1	599	328 (54.8)	478	132 (27.6)
	2	1016	493 (48.5)	1096	111 (10.1)
	3	883	469 (53.1)	765	148 (19.3)
	4	1192	597 (50.1)	713	202 (28.3)
	5	249	143 (57.4)	738	99 (13.4)
			Group mean (52.8)		Group mean (19.7)
$S_{A59}R$	1	529	291 (55.0)	288	61 (21.2)
	2	97	52 (53.6)	330	44 (13.4)
	3	239	134 (56.1)	259	37 (14.3)
	4	403	208 (51.6)	616	170 (27.6)
	5	326	163 (50.0)	282	80 (28.4)
			Group mean (53.3)		Group mean (21.0)

[a] Mice were inoculated intracranially with 10 PFU of either S_4R or $S_{A59}R$. Animals were sacrificed on day 5 postinfection and perfused, and the brain was fixed in formalin, embedded in paraffin, and sectioned sagittally. Section 1 and 2 are adjacent.

[b] The slides were double-immunostained with anti-MHV-A59 serum and AP14, a monoclonal antibody to MAP2b, or a mouse anti-GFAP antibody. Sagittal sections were coded and systematically examined in a blinded fashion (magnification ×190), and the total number of viral antigen-positive cells and double-positive cells per section was determined. The (%) is the percentage of the total number of viral antigen positive cells counted that were also positive for the indicated marker.

forebrain, hippocampus, and cingulate gyrus than $S_{A59}R$ (Phillips *et al.,* 1999). Increased infection could reflect differences in viral spread in a single cell type or in multiple cell types. To quantitatively compare the cellular tropism of S_4R and $S_{A59}R$, we performed double-label immunofluorescence on sagittal brain sections for viral

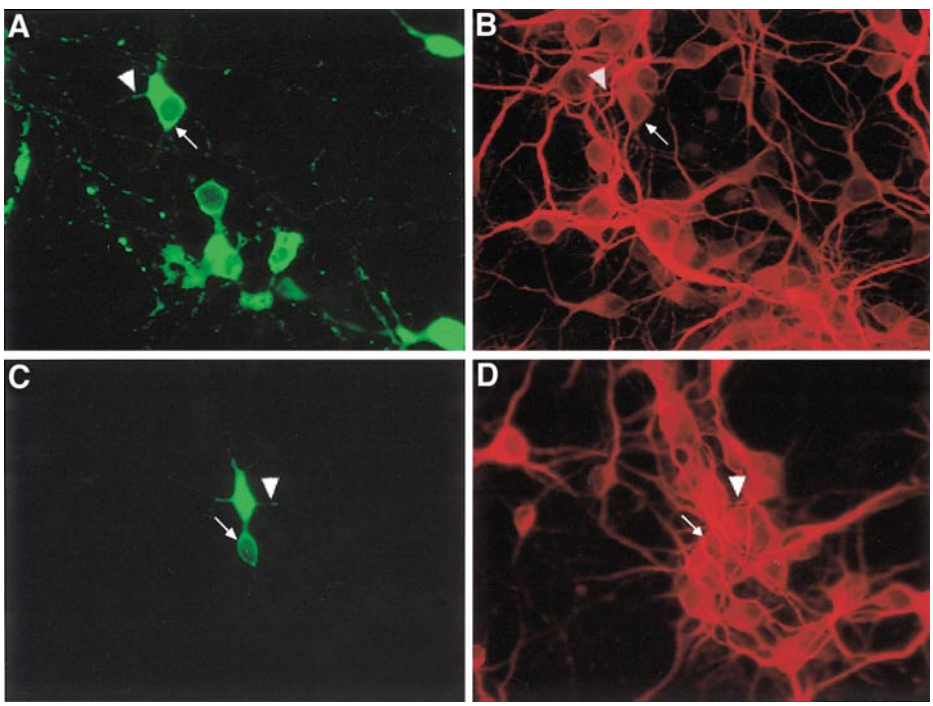

FIG. 3. Viral spread in primary hippocampal neuron cultures. Neurons were cultured for 4 days and then infected with S_4R (A and B) or $S_{A59}R$ (C and D). Representative pictures on day 3 postinfection are shown. Colocalization of viral antigen (A and C) and neuronal cell markers (B and D) were demonstrated using double-immunofluorescence for viral antigen (green) and MAP2 (red). The arrows indicate viral antigen-positive neurons, while the arrowheads indicate viral antigen-positive neurites. Note the large focus of viral antigen-positive cells following infection with S_4R (A). Magnification, ×190.

TABLE 2

S_4R and $S_{A59}R$ Infection of Primary Neuronal Cultures[a]

Virus	Day	Viral titers log (PFU/mL) mean ± SD[b]	No. of foci mean ± SD[c]	No. of viral antigen-positive cells mean ± SD[d]
S4R	0	3.79 ± 0.39	0	0
	1	2.13 ± 0.34	60 ± 17	367 ± 108
	3	2.28 ± 0.22	127 ± 52	842 ± 31
SA59R	0	4.21 ± 0.12	0	0
	1	3.59 ± 0.15	122 ± 79	302 ± 165
	3	3.38 ± 0.19	162 ± 34	471 ± 109

[a] Primary hippocampal neuron cultures were infected on day 4 post-explant at an m.o.i. of 5. Coverslips containing infected neurons were fixed in 2% paraformaldehyde and immunostained for viral antigen (mouse antinucleocapsid).

[b] Supernatants from infected cultures were collected at the indicated times and viral titers were determined on L2 cells. The titers are the mean titers from two independent experiments ($n = 6$).

[c] A group of viral antigen-positive cells that appeared to exhibit cell–cell contact was defined as a focus. The data shown represent the results from two independent experiments ($n = 4$).

[d] The total number of viral antigen-positive cells per coverslip was determined ($n = 4$, except on day 3 following infection with S_4R, $n = 3$). On day 3 the mean number of viral antigen-positive cells was greater following infection with S_4R than $S_{A59}R$ (two-tailed t test, $P < 0.01$).

antigen and MAP2b, a neuron-specific marker (De Camilli *et al.,* 1984; Riederer *et al.,* 1995), or glial fibrillary acidic protein (GFAP), an astrocyte-specific marker. Mice were inoculated intracranially with 10 PFU of S_4R or $S_{A59}R$ and animals were sacrificed at 3 and 5 days postinfection.

The sections were systematically scanned (magnification, ×190) in a blinded fashion, and the total number of viral antigen-positive and double-positive cells was determined. Representative pictures of double-immunofluorescence for viral antigen and MAP2b are shown (Fig. 1). On days 3 and 5 postinfection, the mean number of viral antigen-positive cells per brain section was significantly greater following infection with S_4R than $S_{A59}R$ (two-tailed t test, day 3, $P < 0.05$, and day 5, $P < 0.001$) (Fig. 2). The pattern of viral antigen expression in the brain was similar following infection with S_4R or $S_{A59}R$.

Despite the difference in the absolute number of infected cells, S_4R had a similar cellular tropism as $S_{A59}R$. As shown in Table 1, we found that the percentage of viral antigen-positive cells that were also positive for neuronal or astrocytic markers was remarkably similar for S_4R and $S_{A59}R$. On day 5 postinfection, neurons appeared to account for approximately 53% of either S_4R- or $S_{A59}R$-infected cells, while astrocytes accounted for approximately 20 or 21% of S_4R- or $S_{A59}R$-infected cells, respectively. Thus the increased neurovirulence of S_4R correlated with increased infection of multiple CNS cell-types, including both neurons and astrocytes.

Viral spread of S_4R and $S_{A59}R$ differs in primary neuronal cultures

The extent of neuronal infection is thought to be a determinant of MHV neurovirulence (Dubois-Dalcq *et al.,* 1982; Fleming *et al.,* 1986; Knobler *et al.,* 1981). As an *in vitro* model of CNS infection and to examine the ability of S_4R and $S_{A59}R$ to spread in neurons, we infected primary hippocampal neuron cultures obtained from B6 mice with the two viruses. Immunostaining for MAP2 and GFAP demonstrated that the cultures consisted primarily of neurons with less than 8% of the cells exhibiting GFAP immunoreactivity (data not shown). On days 0, 1, and 3 after infection, supernatants were titered for infectious virus and the number of viral antigen-positive cells was determined by immunofluorescence. Neurons did not exhibit cytopathic effect for the duration of the experiment as assessed by bright-field microscopy.

To compare the number of cells infected with each virus, we used immunofluorescence to detect viral antigen expression. S_4R and $S_{A59}R$ infection of neurons was confirmed by cell morphology and by double-immunostaining for viral antigen and MAP2 (Fig. 3). Viral antigen-positive cells were often located in discrete foci. Moreover, viral antigen-positive neurites could often be observed between infected cells or between foci of infected cells, suggesting that perhaps one means of viral spread in these cultures was along neurites. To examine the pattern of viral spread in these cultures, we determined the total number of viral antigen-positive cells and the total number of foci of infected cells per coverslip at different time points (Table 2). On day 1 postinfection the average number of foci and the total number of antigen-positive cells was similar following infection with S_4R and $S_{A59}R$. On day 3 postinfection, although the average number of foci was similar, the average number of viral antigen-positive cells was significantly greater following infection with S_4R than $S_{A59}R$ (two-tailed t test, $P < 0.01$). Thus, on day 3 the number of viral antigen-positive cells per focus was greater for S_4R, 5.79 ± 1.15, than $S_{A59}R$, 3.17 ± 1.59 (mean ± SD). The difference in the number of infected cells, despite a similar number of foci, between S_4R and $S_{A59}R$, suggested that S_4R spread faster via cell–cell spread than $S_{A59}R$. Thus, the results in primary neuronal cultures were consistent with the results *in vivo* and suggested that the MHV-4 spike conferred an inherent ability to spread rapidly from cell to cell in the CNS.

Consistent with previous studies in which primary neuronal cultures were infected with MHV (Dubois-Dalcq *et al.,* 1982; Pasick *et al.,* 1994), the amount of infectious virus released into the media was minimal. Following infection with S_4R or $S_{A59}R$, the titers of infectious virus in the supernatants initially dropped, day 0 to day 1 postinfection, and then remained the same from day 1 to day 3 postinfection (Table 2). The inactivation of infectious virus in the residual inoculum most likely accounted for the precipitous drop in

viral titers from day 0 to 1 postinfection. On days 1 and 3, the titers of infectious virus were lower in S_4R-infected cultures than S_{A59}R-infected cultures.

Differences in the composition of the lymphocytic response to infection with S_4R and S_{A59}R

The MHV-4 spike appears to mediate more efficient spread in cells of the CNS than the MHV-A59 spike. Previously we observed a difference in the immune response to infection with S_4R and S_{A59}R by H&E staining. S_4R infection induced a greater infiltration of inflammatory cells into the brain than S_{A59}R infection (Phillips *et al.,* 1999). The immune response to MHV infection is complex, and multiple components of the immune response are required for optimal clearance of infectious virus from the CNS. Therefore, both quantitative and qualitative differences in the antiviral immune response may also contribute to the differential neurovirulence of S_4R and S_{A59}R.

We used flow cytometry to quantitatively compare the composition of the immune response in the brain to infection with S_4R and S_{A59}R. Total brain mononuclear cells were isolated on days 5 and 7 postinfection and were examined for surface expression of CD45 (a marker of nucleated cells of hematopoietic lineage), CD8, CD4, and B220.

At the peak of inflammation, day 7 postinfection, the difference in the total number of inflammatory cells in the brain between S_4R and S_{A59}R was dramatic. The number of immune cells, as determined by CD45 positivity, isolated from each brain following S_4R and S_{A59}R infection was between 1.2×10^6 and 1.1×10^7 cells and was on average fivefold greater following infection with S_4R than S_{A59}R. Representative data are shown in Fig. 4. Flow analysis of brain-derived lymphocytes revealed that the percentage of $CD8^+$ T cells was also greater following infection with the more neurovirulent S_4R as compared with S_{A59}R (Fig. 4B). In contrast, the percentage of cells positive for CD4 or B220 (a B cell marker) was similar following infection with S_4R and S_{A59}R. We next examined the ratio of $CD8^+$ to $CD4^+$ T cells for S_4R and S_{A59}R from four independent experiments. The mean ratio of $CD8^+$ to $CD4^+$ T cells following infection with S_4R, 2.83 ± 0.26 (mean $\pm$ SEM), was significantly greater than the ratio following infection with S_{A59}R, 1.73 ± 0.06 (mean $\pm$ SEM) (two-tailed *t* test, $P < 0.01$) ($n = 4$). Due to the difference in total cells isolated per brain, the estimated numbers of $CD45^+$, $CD4^+$, $CD8^+$, and $B220^+$ cells per mouse brain were between three- and fivefold greater following infection with S_4R than with S_{A59}R (Fig. 4C). Thus, the high neurovirulence of S_4R relative to S_{A59}R was correlated with a greater total number of mononuclear cells in the brain, and a significant increase in the percentage of $CD8^+$ T cells.

On day 5 following infection with either S_4R or S_{A59}R, the magnitude of the inflammatory response to infection in the brain was much less than on day 7 postinfection as previously observed by Haring *et al.* (2001) and Williamson *et al.* (1991). In addition, the numbers of $CD8^+$ or $CD4^+$ T cells in the brain were just above the level of detection. Even on day 5 postinfection, however, the number of immune cells in the brain following infection with S_4R was still greater than following S_{A59}R infection (data not shown).

Functional differences in the T cell response to infection with S_4R and S_{A59}R

In addition to differences in the magnitude and in the composition of the immune response to infection with S_4R and S_{A59}R, we hypothesized that there might be differences in the function of MHV-specific T cells. To compare the frequency of functionally activated, MHV-specific $CD8^+$ and $CD4^+$ T cells in the CNS following infection with S_4R or S_{A59}R, we performed intracellular IFN-γ assays. Brain-derived T cells on day 7 postinfection were isolated and challenged with peptides containing the immunodominant or sub-immunodominant $CD8^+$ T cell epitope, S510 or S598, or the immunodominant $CD4^+$ T cell epitope, M133, and stained for intracellular IFN-γ as described previously (Murali-Krishna *et al.,* 1998).

Representative results are shown in Fig. 5. Following S_4R infection, approximately 13.6 and 9.3% of the $CD8^+$ T cell population in the CNS was S510-specific and S598-specific, respectively. S510 and S598 are the only two known $CD8^+$ T cell epitopes for MHV; therefore, the total frequency of MHV-specific $CD8^+$ T cells in the CNS following S_4R infection was approximately 22.9%. The MHV-A59 spike lacks the immunodominant S510 epitope (Luytjes *et al.,* 1987). Thus, following infection with S_{A59}R the MHV-specific $CD8^+$ T cell response was S598-specific and accounted for approximately 11.8% of the $CD8^+$ T cell response.

Within the population of cells isolated from the CNS, a proportion of $CD4^+$ cells exhibited intracellular IFN-γ in the absence of peptide (Fig. 5B). The reason for this background level of IFN-γ expression is not known; however, it has been suggested that infected microglia and macrophages in the CNS cell preparation may stimulate $CD4^+$ T cells (Haring *et al.,* 2001). The frequency of M133-specific $CD4^+$ T cells following infection with S_4R or S_{A59}R was similar, accounting for approximately 16.0 and 15.4% of the $CD4^+$ T cell response, respectively. As this may overestimate the frequency of MHV-specific cells in the CNS, we also subtracted the percentage of IFN-γ-expressing cells in the absence of peptide from the total percentage of IFN-γ-expressing cells after peptide stimulation. The calculated frequency of M133-specific $CD4^+$ T cells following infection with S_4R, 10.6%, and S_{A59}R, 8.9%, was also similar. Thus, infection with either S_4R or S_{A59}R resulted in a robust $CD8^+$ and $CD4^+$ T cell

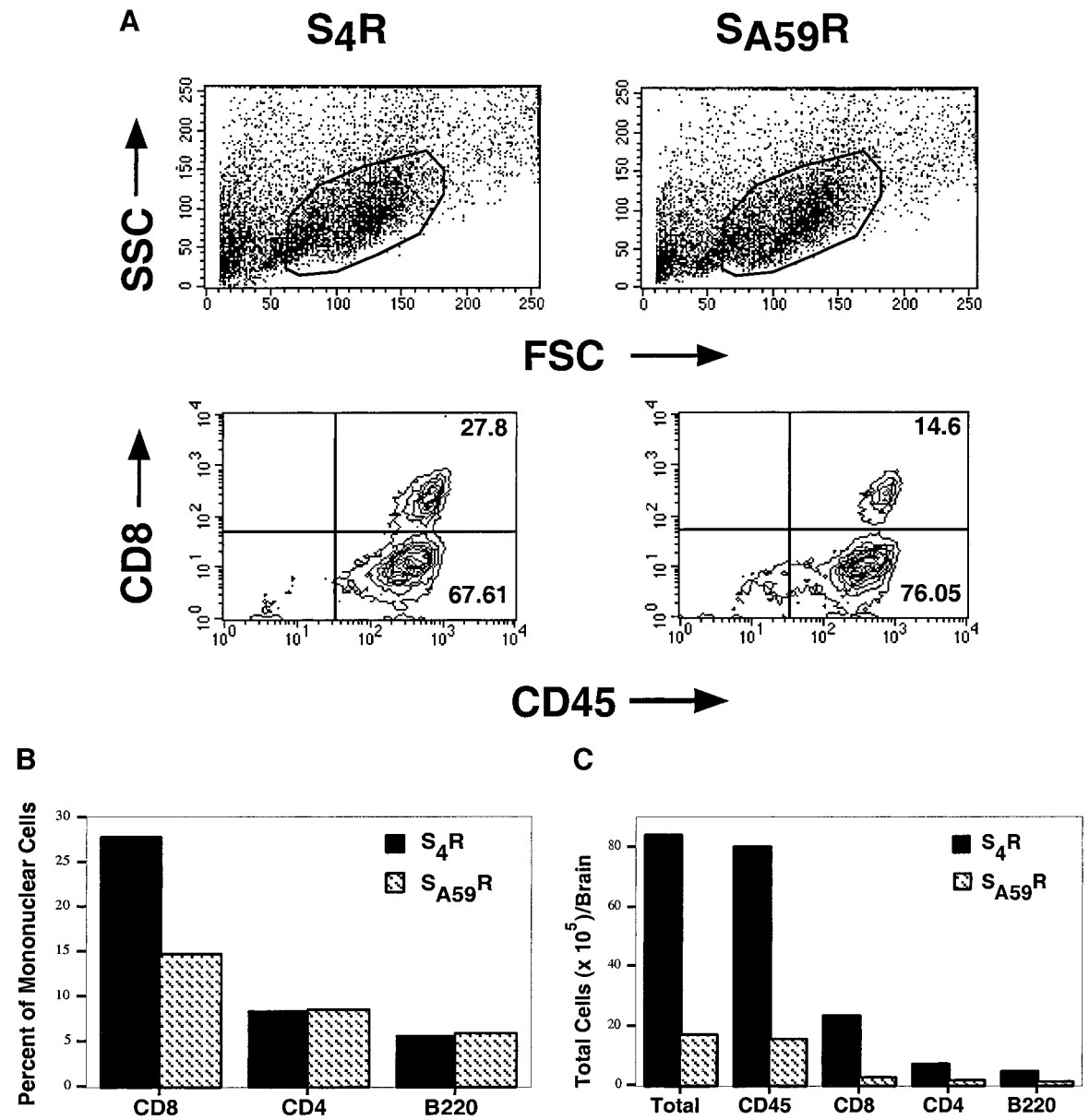

FIG. 4. Lymphocyte populations in the brain following inoculation with S_4R and $S_{A59}R$. Mice were infected with S_4R or $S_{A59}R$ and animals were sacrificed at the peak of inflammation, day 7 postinfection. (A) The upper row depicts the forward scatter and side scatter characteristics of representative mononuclear cell preparations from the brains of S_4R- and $S_{A59}R$-infected mice. Surface expression of CD45 was used to assist in the gating of mononuclear cells, and representative flow cytometry density plots showing expression of CD45 (*x*-axis) and CD8 (*y*-axis) in S_4R-infected mice (left lower row) and $S_{A59}R$-infected mice (right lower row). Numbers in the upper right quadrants represent the percentage of $CD8^+$ $CD45^+$ monocytes, and the numbers in the right lower quadrant represent the percentage of $CD8^-$ $CD45^+$ monocytes. (B) Relative percentages of $CD8^+$, $CD4^+$, and $B220^+$ cells in brain-derived monocytes. (C) Absolute numbers of total cells, $CD45^+$, $CD8^+$, $CD4^+$, and $B220^+$ cells in cell preparations from the brain. Mononuclear cell preparations from six mice were pooled, and the results are representative of four independent experiments. A smaller number of cells (6.6×10^5 cells per brain) were obtained from mock-infected mice with only 4% of these $CD45^+$.

response that was both epitope-specific and functional. The major difference between the frequency of virus-specific T cells induced by S_4R and $S_{A59}R$ was the increased frequency of functionally activated $CD8^+$ T cells following infection with the more neurovirulent S_4R. Note that due to the increased numbers of inflammatory cells in the brain following S_4R infection relative to $S_{A59}R$ infection, the total number of virus-specific $CD8^+$ and $CD4^+$ T cells in the brain was greater following infection with S_4R than $S_{A59}R$.

Contribution of lymphocytes to differential neurovirulence

S_4R infection resulted in a greater number of lymphocytes and a higher frequency of virus-specific immune

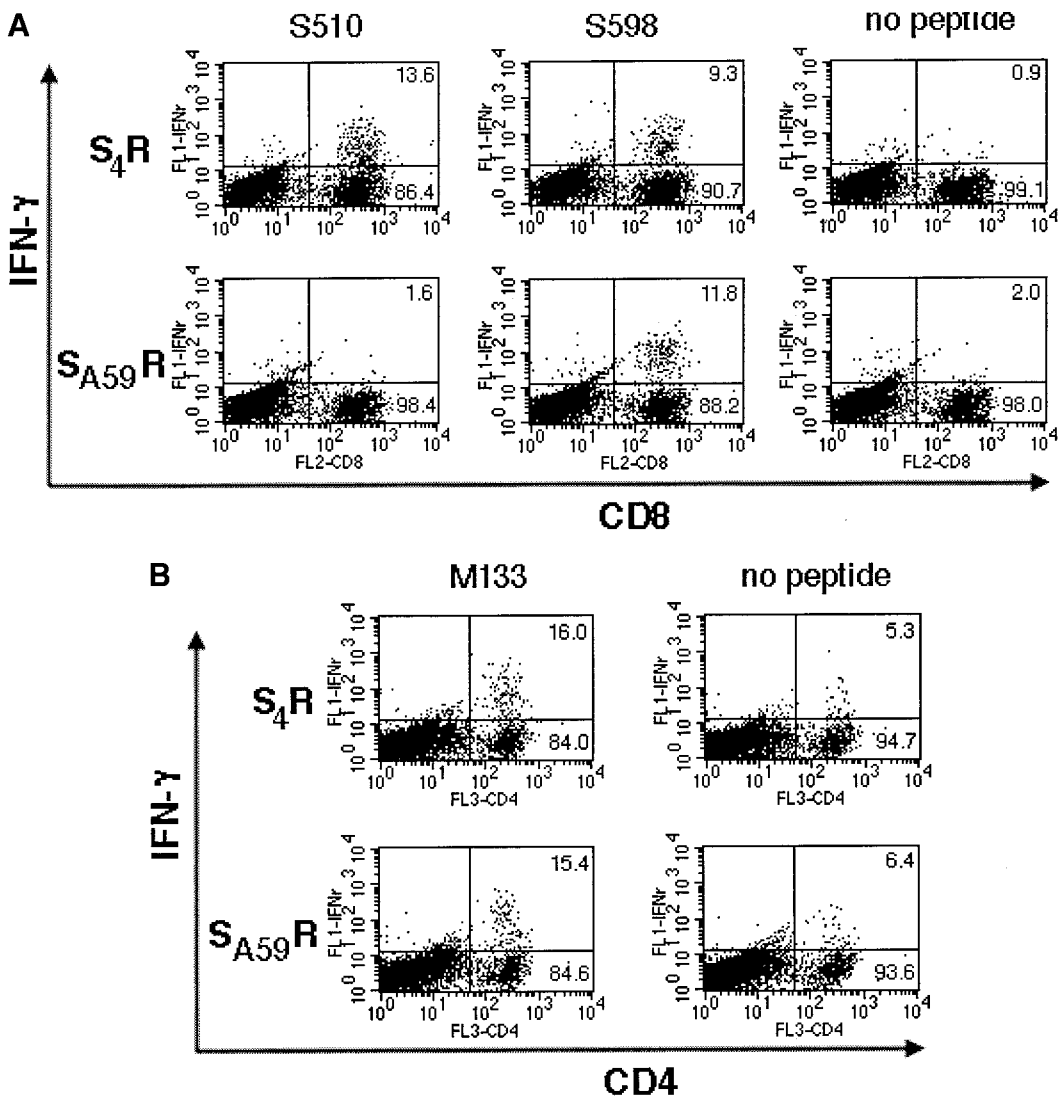

FIG. 5. MHV-specific $CD8^+$ and $CD4^+$ T cells following infection with S_4R and $S_{A59}R$. Mononuclear cells were isolated from the brain of S_4R- and $S_{A59}R$-infected mice on day 7 postinfection, and the frequency of $CD8^+$ and $CD4^+$ T cells specific for MHV-specific epitopes were determined by intracellular IFN-γ staining. Cells were cultured with or without peptide as indicated above each column. The numbers in the upper right quadrants indicate the percentage of $CD8^+$ T cells (A) or $CD4^+$ T cells (B) that are positive for the intracellular IFN-γ stain following infection with either S_4R (top row) or $S_{A59}R$ (bottom row). The numbers in the right lower quadrants represent the percentage of $CD8^+$ T cells (A) or $CD4^+$ T cells (B) that are negative for the intracellular IFN-γ stain. Brain mononuclear cells were pooled from six to eight animals, and these data are representative of two to five experiments.

cells in the CNS than $S_{A59}R$ infection. To evaluate the contribution of lymphocytes to the differential neurovirulence observed with S_4R and $S_{A59}R$, we compared the survival of infected RAG1−/− mice (B6 background), which lack functional T and B cells (Mombaerts *et al.,* 1992), and immunocompetent B6 mice. RAG1−/− mice infected with $S_{A59}R$ experienced 100% mortality while immunocompetent mice survived following challenge with $S_{A59}R$ (Fig. 6A). Thus, $S_{A59}R$-infected immunocompetent B6 mice are protected from death by the activated immune response, and without this response the mice succumb to a lethal infection. In contrast, RAG1−/− mice infected with S_4R exhibited prolonged survival relative to immunocompetent B6 mice: the median survival time for S_4R-infected mice was 13 days in RAG1−/− and 10 days in B6 mice (statistically different, Mann–Whitney rank sum test, $P < 0.0001$) (Fig. 6B). Prolonged survival in S_4R-infected RAG1−/− mice suggested that T or B cells contributed to pathology.

We examined virus titers in the brain and other organs of RAG1−/− mice. At five days postinfection, the titers of infectious virus in the brains of RAG1−/− mice were similar to those in B6 mice, following $S_{A59}R$ infection 6.0 vs 5.4 and following S_4R infection 5.1 vs 5.1 [$\log_{10}$(PFU/g)] ($n = 2$), respectively. In addition, similar to the infection in immunocompetent mice the level of infectious virus was minimal in the liver and undetectable in the spleen, kidney, lung, heart, and a portion of the small intestine

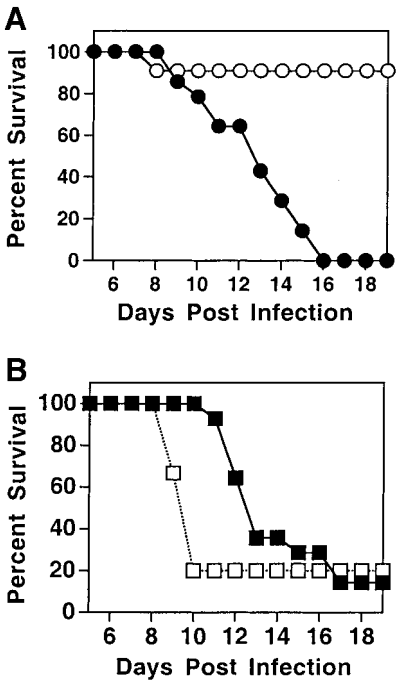

FIG. 6. Effect of a functional T and B cell response on mortality following intracranial inoculation with $S_{A59}R$ (A) or S_4R (B). B6 (open symbols) or RAG1−/− (closed symbols) mice were inoculated with 10 PFU of virus and observed daily for mortality. The percentage survival and median time to death in days (number to right of line) is shown. Following inoculation with S_4R (B), there was a significant difference in the median time to death between RAG1−/− and B6-infected mice (13 and 10 days, respectively, Mann–Whitney rank sum test, $P < 0.0001$). Although not shown on the graph, all RAG1−/− mice inoculated with S_4R died by 43 days postinfection. No deaths were observed in B6 mice after 19 days postinoculation. The data shown represent the results from two independent experiments from a total of 14 RAG1−/− mice per virus, 11 B6 mice inoculated with $S_{A59}R$, and 15 B6 mice inoculated with S_4R.

(data not shown). Unlike B6 mice, which clear infectious virus early in infection, by day 13 postinfection with S_4R or $S_{A59}R$ there were high levels of infectious virus in the brain. Infectious virus remained localized to the CNS following S_4R infection, but mice infected with $S_{A59}R$ had high titers of virus in the spleen and liver at late times postinfection (data not shown). Thus, following infection with $S_{A59}R$ the acquired immune response was critical for viral clearance in the brain, protection from viral spread to other organs, and protection from subsequent death. In contrast, S_4R-infected RAG1−/− mice displayed prolonged survival despite persistent, high titers of infectious virus in the CNS, suggesting that immune-mediated pathology may contribute to the highly neurovirulent phenotype of S_4R.

DISCUSSION

The spike glycoprotein is a major determinant of MHV neurovirulence. We examined how alterations in spike affect neuropathogenesis using S_4R and $S_{A59}R$, two isogenic recombinant viruses that differ exclusively in spike. To identify the parameters of MHV infection mediated by spike and important in neurovirulence, we compared the cellular tropism of S_4R and $S_{A59}R$ and both quantitative and functional features of the immune response to infection. Our studies suggest that differences in viral spread in multiple cell types, differences in the magnitude of the immune response to infection, and immune-mediated pathology contribute to the differential neurovirulence of S_4R and $S_{A59}R$. We have shown previously (Phillips *et al.,* 1999, 2001) that, during acute infection, the titers of infectious virus in the brains of animals infected with S_4R and $S_{A59}R$ are similar. Thus, the spread of viral antigen, neurovirulence, and mortality are not determined by the level of infectious virus in the CNS.

Neuronal infection has been proposed to be a major determinant of MHV neurovirulence (Dubois-Dalcq *et al.,* 1982; Fleming *et al.,* 1986; Knobler *et al.,* 1981). Using double-immunohistochemistry, we quantitatively compared the tropism of S_4R and $S_{A59}R$ for neurons and astrocytes. We determined that on days 3 and 5 postinfection, S_4R infected a greater total number of cells than $S_{A59}R$ throughout the brain. Despite the difference in viral spread, however, the tropism of S_4R and $S_{A59}R$ for neurons and astrocytes was identical. Thus differences in viral spread, not differences in neuronal tropism per se, contributed to the differential neurovirulence of S_4R and $S_{A59}R$.

Despite the similarity in neuronal tropism, however, the number of infected neurons was greater following infection with S_4R than $S_{A59}R$ due to the greater total number of cells infected. To compare the ability of S_4R and $S_{A59}R$ to spread in cells from the CNS, we examined the infection of primary hippocampal neuron cultures. S_4R infection of neuronal cultures resulted in greater viral spread than $S_{A59}R$ infection, and the pattern of spread suggested that S_4R spreads more rapidly from cell to cell than $S_{A59}R$. Viral spread along neuronal processes could contribute to rapid dissemination of virus to multiple regions of the brain. Future studies will address how the MHV-4 spike confers rapid cell to cell spread, and the effect of infection on neuronal viability.

In addition to increased viral spread, S_4R mediated a greater influx of immune cells into the CNS than $S_{A59}R$. To identify how this increased immune response to infection might influence the differential neurovirulence of S_4R and $S_{A59}R$, we compared the composition and the function of the lymphocytic response to infection. At the peak of inflammation, day 7 after infection, the more neurovirulent S_4R induced the infiltration of a greater number of T cells and B cells into the CNS with a specific increase in the percentage of $CD8^+$ T cells as compared to $S_{A59}R$.

We also compared the virus-specific activity of $CD4^+$ and $CD8^+$ T cells from the CNS of animals infected with S_4R and $S_{A59}R$ by measuring intracellular IFN-γ secretion

in response to specific viral epitopes. Both S_4R and $S_{A59}R$ induced robust and virus-specific immune responses; however, there were differences in the specificity of the $CD8^+$ T cell response. The two H-2^b $CD8^+$ T cell epitopes recognized in B6 mice are located in the spike glycoprotein at residues 510–518 (S510) and 598–605 (S598) (Bergmann *et al.,* 1996; Castro and Perlman, 1995). A 52 amino acid deletion in the spike of MHV-A59 relative to the spike of MHV-4 removes the more immunodominant 510–518 epitope (Luytjes *et al.,* 1987; Parker *et al.,* 1989). Consistent with this difference in epitopes, the frequency of S510-specific $CD8^+$ T cells in the CNS was high following S_4R infection and undetectable following $S_{A59}R$ infection. The lack of the S510 epitope in $S_{A59}R$ did not appear to induce a significantly greater immune response to S598, however, as the frequency of S598-specific $CD8^+$ T cells in the CNS following infection with S_4R or $S_{A59}R$ was similar. The two viruses also shared a similar frequency of response to the dominant $CD4^+$ T cell epitope (Xue and Perlman, 1997), M133, located within the viral matrix protein.

Thus, expression of the S510 epitope was responsible for the greatest difference in the frequencies of virus-specific, functionally activated T cells following infection with S_4R and $S_{A59}R$. S_4R infection induced a greater percentage of $CD8^+$ T cells in the CNS than $S_{A59}R$ infection. The response to the S510 epitope in the S_4R spike may at least partially account for this increase in the frequency of $CD8^+$ T cells. Interestingly, mutations in the S510 epitope in a related MHV-JHM strain have been associated with alterations in neuropathogenesis (Pewe *et al.,* 1998). However there are other factors that may contribute. For example, quantitative differences in antigen presentation or differences in the ability of immune cells to traffic to and proliferate in the CNS following infection with S_4R and $S_{A59}R$ may contribute to differences in the percentage of $CD8^+$ T cells and to the overall magnitude of the antiviral immune response. Furthermore the percentage of total $CD8^+$ T cells among CNS lymphocytes (Fig. 4) may include $CD8^+$ cells specific for epitopes other than S510 and S598, perhaps host epitopes. Future experiments will address the role of this epitope in the differential neurovirulence of S_4R and $S_{A59}R$.

To examine the role of the T and B cell response to infection in the differential neurovirulence of S_4R and $S_{A59}R$, we compared the virulence of these viruses in the presence and absence of a functional T and B cell response. Despite prolonged replication of infectious S_4R in the CNS of RAG−/− mice, these mice exhibited prolonged survival relative to immunocompetent mice. In contrast, the T and B cell response to $S_{A59}R$ infection was primarily protective. These data suggest that immune-mediated pathology contributes to the high neurovirulence of S_4R. Interestingly, previous studies with MHV have also suggested that, in addition to its role in protection, the inflammatory response, particularly the T cell response, can be immunopathologic. Prolonged survival of perforin-deficient mice infected with a JHM strain of virus suggested that $CD8^+$ CTLs might contribute to disease (Lin *et al.,* 1997). Moreover, $CD4^+$ T cells have also been implicated in immunopathology; both adoptive transfer experiments with $CD4^+$ T cells and infection of $CD4^+$ knockout mice have suggested that $CD4^+$ T cells in the CNS may increase disease morbidity (Lane *et al.,* 2000; Wu *et al.,* 2000). To determine whether $CD8^+$ or $CD4^+$ T cells were primarily responsible for the prolonged survival in RAG−/− mice, we compared the survival of CD8−/−, CD4−/−, and immunocompetent B6 mice infected with S_4R; however, the absence of either T cell subset alone did not confer significantly increased survival (data not shown).

Previous studies have demonstrated the complexity of the immune response to MHV and the requirement for multiple components for clearance (Korner *et al.,* 1991; Stohlman *et al.,* 1986, 1995, 1998; Sussman *et al.,* 1989; Williamson and Stohlman, 1990; Yamaguchi *et al.,* 1991; Bergmann *et al.,* 2001). Our results suggest that MHV-induced immunopathology is also complex and involves multiple components of the immune response to infection. Studies with LCMV and HIV have suggested that virus strains that exhibit rapid viral spread are associated with increased immune-mediated pathology (Wodarz and Krakauer, 2000; Moskophidis *et al.,* 1995). Future studies will delineate which components of the immune response to S_4R contribute to immunopathology and examine how increased viral spread may induce such a response.

Increased neurovirulence conferred by the MHV-4 spike correlates with both rapid viral spread in the CNS and immune-mediated pathology. By studying two isogenic viruses with defined alterations in spike in *in vivo* infections and in *in vitro* models of MHV infection, we can begin to dissect the different roles of the spike glycoprotein in neurovirulence. Furthermore, we can examine the contribution of virus- and immune-mediated pathology to neurovirulence.

MATERIALS AND METHODS

Virus and cells

The recombinant viruses, referred to as S_4R (containing the MHV-4 spike gene) or $S_{A59}R$ (containing the MHV-A59 spike gene), were generated using targeted RNA recombination and are in the MHV-A59 background (Fischer *et al.,* 1997). We have in the past described independent isolates of both S_4R (S_4R22 and S_4R29) and $S_{A59}R$ [$S_{A59}R13$ (wtR13) and $S_{A59}R16$] (Phillips *et al.,* 1999, 2001). Since the group of recombinant viruses expressing the MHV-4 spike gene are phenotypically indistinguishable from each other, they will be referred to collectively as S_4R; similarly, since the group of viruses

expressing the A59 spike gene are phenotypically indistinguishable from each other, they will be referred to collectively as $S_{A59}R$. All viral stocks were grown in 17Cl-1 cells, and infectious virus was quantified by plaque assay, using murine L2 cells as indicator cells.

Inoculation of mice

Four-week old male C57Bl/6 (B6) mice were purchased from the National Cancer Institute (Bethesda, MD), and four-week old male RAG1−/− mice were purchased from the Jackson Laboratory (Bar Harbor, ME). No mature B or T lymphocytes are produced in RAG1−/− mice (Mombaerts *et al.,* 1992). All mice were certified MHV-free. Mice were anesthetized with Isoflurane (IsoFlo; Abbott Laboratories), and injections were performed in the left cerebral hemisphere. Each injection contained 10 PFU of virus diluted to a volume of 20 μl per mouse in PBS containing 0.75% bovine serum albumin. Mock-infected controls were inoculated similarly but with an uninfected 17Cl-1 cell lysate at a comparable dilution.

Double-label indirect immunofluorescence on brain sections

At various times after infection with S_4R or $S_{A59}R$, mice were sacrificed and perfused with 10 ml of PBS, and the brains were removed. The right half of the brain was fixed in Formalin for 2 days, embedded in paraffin, sectioned, and left unstained for immunofluorescence. Adjacent sagittal brain sections close to midline, 10–20 μm apart, were examined. Sections were blocked with 2% goat serum in Tris–HCl and 0.1% Triton X-100 for 1 h, incubated with primary antibodies for 2 h, and incubated with secondary antibodies for 1 h. All incubations were carried out in a humidified chamber at 37°C, and after each step the sections were washed (three times for 5 min each) in PBS. For localization of viral antigen, sections were incubated with a 1:100 dilution of rabbit anti-MHV-A59 serum, made against detergent-disrupted MHV-A59, obtained from Mark Denison (Vanderbilt University, TN). Neurons were identified with a 1:50 dilution of mouse monoclonal antibody AP14 (Geisert *et al.,* 1990), which recognizes the MAP2b protein (De Camilli *et al.,* 1984; Riederer *et al.,* 1995), obtained from Virginia M.-Y. Lee (University of Pennsylvania, PA). Astrocytes were identified with a 1:50 dilution of a mouse monoclonal antiglial fibrillary acidic protein (PharMingen). Rabbit antibodies were detected with a 1:40 dilution of TRITC-conjugated swine anti-rabbit immunoglobulins (Dako Corp.). Murine antibodies were detected with a 1:100 dilution of biotin-conjugated horse anti-mouse immunoglobulins followed by treatment with a 1:200 dilution of Fluorescein Avidin D (FITC) for 30 min, purchased from Vector Laboratories.

Control slides were incubated in parallel with preimmune rabbit serum, and sections from mock-infected animals were incubated with rabbit anti-MHV-A59 serum. For each double-immunostaining scheme, it was verified that the secondary antibody did not bind in the absence of the primary antibody or cross-react with primary antibodies of different species.

Isolation of primary hippocampal neurons

Primary hippocampal neurons were obtained from day 14 to day 16 embryonic mice, as described previously (Banker and Goslin, 1991; Pasick *et al.,* 1994; Rall *et al.,* 1997), except the cells were maintained in neurobasal medium (Gibco/BRL) containing 4 μg/ml glutamate, in the absence of an astrocyte feeder layer. The mice used in these experiments were C57Bl/6 transgenic mice expressing the human MV receptor, CD46 (Rall *et al.,* 1997). Cells were plated at a density of $2–7 \times 10^5$ cells per glass coverslip.

Infection of primary hippocampal neuron cultures and virus detection

On day 4 postexplant, cells were infected at a multiplicity of infection (m.o.i.) of 5 with S_4R or $S_{A59}R$ or mock-infected with 17Cl-1 cell lysate. After 1 h at 37°C with gentle agitation, the inoculum was removed; conditioned neurobasal medium was added back to the cultures, and the cultures were maintained at 37°C in 5% CO_2 until harvesting. In each of two independent experiments three coverslips were infected per virus per time point.

The levels of infectious virus in the supernatants as a function of time following infection were determined by plaque-assay on L2 cell monolayers. For the localization of viral antigen coverslips containing infected cells were washed once with PBS, fixed in 1% paraformaldehyde, and stored at 4°C. Coverslips were blocked with 2% goat serum in Tris–HCl and 0.1% Triton X-100 for 15 min, incubated with primary antibodies for 2 h, and incubated with secondary antibodies for 1 h. Between each step the coverslips were washed in Tris–HCl and 0.1% Triton X-100 six times, and all incubations were carried out at room temperature in a humidified chamber. To detect viral antigen coverslips were incubated with a 1:20 dilution of mouse antinucleocapsid antibody, obtained from Julian L. Leibowitz (Texas A&M University, TX). This was followed by incubation with the secondary antibody, a 1:200 dilution of biotin-conjugated horse anti-mouse immunoglobulins (Vector Laboratories), and then incubation with a 1:200 dilution of fluorescein avidin D (FITC) (Vector Laboratories) for 30 min. MAP2 and GFAP were detected with a 1:300 dilution of rabbit anti-MAP2 obtained from Virginia M.-Y. Lee (University of Pennsylvania, PA) and a 1:250 dilution of rabbit anti-cow glial fibrillary acidic protein (GFAP) (Dako Corp.), respectively. Rabbit antibodies were detected with a 1:40 dilution of TRITC-conjugated swine anti-rabbit immunoglobulins (Dako

Corp.). Mock-infected coverslips were incubated in parallel with mouse antinucleocapsid antibodies. Coverslips mounted on slides were blinded and systematically examined by fluorescence and bright-field microscopy (magnification, ×190 and ×380).

Isolation of monocytes from the CNS

Monocytes were prepared from the CNS as previously described by Pewe *et al.* (1999) on days 5 and 7 after intracranial inoculation with 10 PFU of S_4R or S_{A59}R or mock-infected with 17Cl-1 cell lysate. Two to six brains were pooled per sample. In brief, animals were sacrificed and perfused with 10 mL of PBS, and a single-cell suspension from the brain was obtained by passing cells through a nylon mesh bag (64-μm pore diameter). Percoll (Pharmacia) was added to a final concentration of 30%, and the lysate was centrifuged at 1300 *g* for 30 min at 4°C. The cell pellet was resuspended, passed through a cell strainer (pore diameter, 70 μm) (Becton–Dickinson), and washed. The cells were then layered over 2 ml Lympholyte-M (Cedarlane Laboratories) and centrifuged at 1300 *g* for 20 min at room temperature. Cells were removed from the interface, washed once, and counted.

Flow analysis

Expression of cell-surface markers was determined by staining cells with monoclonal antibodies specific for CD8a (clone 53–6.7), CD4 (clone RM4-5), CD45 (leukocyte common antigen, clone 30-F11), and B220 (CD45R/B220, clone RA3-6B2) purchased from PharMingen. For flow cytometry approximately 1×10^6 cells were washed three times with PBS 1% BSA and blocked with 50 μg of rat IgG and a 1:200 dilution of anti-CD16/CD32 (FcγIII/II receptor, clone 2.4G2). Cells were then surface stained for the appropriate markers for 1 h at 4°C, washed three times with PBS 1% BSA, and fixed in 2% paraformaldehyde. Cells were analyzed using a FACScan flow cytometer (Becton–Dickinson). The total number of cells positive for each marker per mouse was determined by multiplying the fraction of cells positive for the marker by the total number of live cells isolated per brain. As controls, monocytes were incubated with isotype controls and monocytes from the brains of mock-infected mice were incubated with antibodies to cell markers.

Intracellular IFN-γ staining

Intracellular IFN-γ expression in response to peptide stimulation was performed as previously described (Murali-Krishna *et al.,* 1998). We cultured 1×10^6 brain-derived monocytes/well for 5 h at 37°C in 200 μl of RPMI 1640 complete supplemented with 5% FCS, 10 units human recombinant IL-2, and 1 μl/ml Brefeldin A (Golgistop, PharMingen) either with or without epitope peptides. The peptides were used at a concentration of 0.1 μg/ml. Cells were then stained as above for surface expression of CD8 or CD4 and incubated overnight at 4°C. For intracellular IFN-γ staining cells were then fixed and permeabilized using the Cytofix/Cytosperm kit (PharMingen), and stained with a FITC-conjugated monoclonal rat anti-mouse IFN-γ antibody (clone XMG 1.2, PharMingen).

Survival assays

RAG1−/− and B6 mice were inoculated intracranially with10 PFU of S_4R or S_{A59}R. In two independent experiments, a total of 14 RAG1−/− mice were analyzed per virus, and in parallel a total of 11 B6 mice inoculated with S_{A59}R and 15 B6 mice inoculated with S_4R were analyzed. Mice were examined for signs of disease or death on a daily basis up to 21 days postinfection, after which they were examined every fourth day, and the percentage survival was calculated.

ACKNOWLEDGMENTS

This work was supported by Public Health Service Grants NS-30606 and NS-21954, and a National Multiple Sclerosis Society Grant RG-2585. J.J.P. was supported in part by Training Grant GM-07229. We thank Virginia M.-Y. Lee for antibodies against neuronal markers, Mark Denison for anti-MHV-A59 serum, Julian L. Leibowitz for antinucleocapsid antibody, Amy Matthews (and other members of Y. Paterson lab) for reagents and helpful advice, Lecia Pewe for helpful advice with flow analysis, and Jean Tsai for providing S_{A59}R16. We also thank Dennis L. Kolson for advice throughout the project and critical reading of the manuscript.

REFERENCES

Banker, G., and Goslin, K. (1991). "Culturing Nerve Cells" (G. Banker, and K. Goslin, Eds.), pp. 251–281. MIT Press, Cambridge, MA.

Bergmann, C. C., Yao, Q., Lin, M., and Stohlman, S. A. (1996). The JHM strain of mouse hepatitis virus induces a spike protein-specific D^b-restricted cytotoxic T cell response. *J. Gen. Virol.* **77,** 315–325.

Bergmann, C. C., Ramakrishna, C., Kornacki, M., and Stohlman, S. A. (2001). Impaired T cell immunity in B cell-deficient mice following viral central nervous system infection. *J. Immunol.* **167,** 1575–1583.

Boyle, J. F., Weismiller, D. G., and Holmes, K. V. (1987). Genetic resistance to mouse hepatitis virus correlates with the absence of virus-binding activity on target tissues. *J. Virol.* **61,** 185–189.

Castro, R. F., and Perlman, S. (1995). CD8+ T-cell epitopes within the surface glycoprotein of a neurotropic coronavirus and correlation with pathogenicity. *J. Virol.* **69,** 8127–8131.

Collins, A. R., Knobler, R. L., Powell, H., and Buchmeier, M. J. (1982). Monoclonal antibodies to murine hepatitis virus-4 (strain JHM) define the viral glycoprotein responsible for attachment and cell-cell fusion. *Virology* **119,** 358–371.

De Camilli, P., Miller, P. E., Navone, F., Theurkauf, W. E., and Vallee, R. B. (1984). Distribution of microtubule-associated protein 2 in the nervous system of the rat studied by immunofluorescence. *Neuroscience* **11,** 817–846.

Dubois-Dalcq, M. E., Doller, E. W., Haspel, M. V., and Holmes, K. V. (1982). Cell tropism and expression of mouse hepatitis viruses (MHV) in mouse spinal cord cultures. *Virology* **119,** 317–331.

Fischer, F., Stegen, C. F., Koetzner, C. A., and Masters, P. S. (1997). Analysis of a recombinant mouse hepatitis virus expressing a foreign gene reveals a novel aspect of coronavirus transcription. *J. Virol.* **71,** 5148–5160.

Fleming, J. O., Trousdale, M. D., El-Zaatari, F. A. K., Stohlman, S. A., and

Weiner, L. P. (1986). Pathogenicity of antigenic variants of murine coronavirus JHM selected with monoclonal antibodies. *J. Virol.* **58,** 869–875.

Geisert, E. E., Jr., Johnson, H. G., and Binder, L. I. (1990). Expression of microtubule-associated protein 2 by reactive astrocytes. *Proc. Natl. Acad. Sci. USA* **87,** 3967–3971.

Haring, J. S., Pewe, L. L., and Perlman, S. (2001). High-magnitude, virus-specific CD4 T-cell response in the central nervous system of Coronavirus-infected mice. *J. Virol.* **75,** 3043–3047.

Knobler, R. L., Dubois-Dalcq, M., Haspel, M. V., Claysmith, A. P., Lampert, P. W., and Oldstone, M. B. (1981). Selective localization of wild type and mutant mouse hepatitis virus (JHM strain) antigens in CNS tissue by fluorescence, light and electron microscopy. *J. Neuroimmunol.* **1,** 81–92.

Korner, H., Schliephake, A., Winter, J., Zimprich, F., Lassman, H., Sedgwick, J., Siddell, S. G., and Wege, H. (1991). Nucleocapsid or spike protein-specific CD4+ T lymphocytes protect against coronavirus induced encephalomyelitis in the absence of CD8+ cells. *J. Immunol.* **147,** 2317–2323.

Lane, T. E., Liu, M. T., Chen, B. P., Asensio, V. C., Samawi, R. M., Paoletti, A. D., Campbell, I. L., Kunkel, S. L., Fox, H. S., and Buchmeier, M. J. (2000). A central role for CD4(+) T cells and RANTES in virus-induced central nervous system inflammation and demyelination. *J. Virol.* **74,** 1415–1424.

Lavi, E., Gilden, D. H., Wroblewska, Z., Rorke, L. B., and Weiss, S. R. (1984). Experimental demyelination produced by the A59 strain of mouse hepatitis virus. *Neurology* **34,** 597–603.

Lavi, E., Fishman, P. S., Highkin, M. K., and Weiss, S. R. (1988). Limbic encephalitis after inhalation of a murine coronavirus. *Lab. Invest.* **58,** 31–36.

Lin, M. T., Stohlman, S. A., and Hinton, D. R. (1997). Mouse hepatitis virus is cleared from the central nervous systems of mice lacking perforin-mediated cytolysis. *J. Virol.* **71,** 383–391.

Luytjes, W., Sturman, L. S., Bredenbeck, P. J., Charite, J., van der Zeijst, B. A. M., Horzinek, M. C., and Spaan, W. J. M. (1987). Primary structure of the glycoprotein E2 of coronavirus MHV-A59 and identification of the trypsin cleavage site. *Virology* **161,** 479–487.

Mombaerts, P., Iacomini, J., Johnson, R. S., Herrup, K., Tonegawa, S., and Papaioannou, V. E. (1992). RAG-1-deficient mice have no mature B and T lymphocytes. *Cell* **68,** 869–877.

Moskophidis, D., Battegay, M., van den Broek, M., Laine, E., Hoffmann-Rohrer, U., and Zinkernagel, R. M. (1995). Role of virus and host variables in virus persistence or immunopathological disease caused by a non-cytolytic virus. *J. Gen. Virol.* **76,** 381–391.

Murali-Krishna, K., Altman, J. D., Suresh, M., Sourdive, D. J. D., Zajac, A. J., Miller, J. D., Slansky, J., and Ahmed, R. (1998). Counting antigen-specific CD8 T cells: A reevaluation of bystander activation during viral infection. *Immunity* **8,** 177–187.

Parker, S. E., Gallagher, T. M., and Buchmeier, M. J. (1989). Sequence analysis reveals extensive polymorphism and evidence of deletions within the E2 glycoprotein gene of several strains of murine hepatitis virus. *Virology* **173,** 664–673.

Pasick, J. M., Kalicharran, K., and Dales, S. (1994). Distribution and trafficking of JHM coronavirus structural proteins and virions in primary neurons and the OBL-21 neuronal cell line. *J. Virol.* **68,** 2915–2928.

Pewe, L., Xue, S., and Perlman, S. (1998). Infection with cytotoxic T-lymphocyte escape mutants results in increased mortality and growth retardation in mice infected with a neurotropic coronavirus. *J. Virol.* **72,** 5912–5918.

Pewe, L., Heard, S. B., Bergmann, C., Dailey, M. O., and Perlman, S. (1999). Selection of CTL escape mutants in mice infected with a neurotropic coronavirus: Quantitative estimate of TCR diversity in the infected central nervous system. *J. Immunol.* **163,** 6106–6113.

Phillips, J. J., Chua, M. M., Lavi, E., and Weiss, S. R. (1999). Pathogenesis of chimeric MHV4/MHV-A59 recombinant viruses: The murine coronavirus spike protein is a major determinant of neurovirulence. *J. Virol.* **73,** 7752–7760.

Phillips, J. J., Chua, M. M., Seo, S.-H., and Weiss, S. R. (2001). Multiple regions of the murine coronavirus spike glycoprotein influence neurovirulence. *J. Neurovirol.* **7,** 421–431.

Rall, G. F., Manchester, M., Daniels, L. R., Callahan, E. M., Belman, A. R., and Oldstone, M. B. (1997). A transgenic mouse model for measles virus infection of the brain. *Proc. Natl. Acad. Sci. USA* **94,** 4659–4663.

Riederer, B. M., Draberova, E., Viklicky, V., and Draber, P. (1995). Changes of MAP2 phosphorylation during brain development. *J. Histochem. Cytochem.* **43,** 1269–1284.

Stohlman, S. A., Matsushima, G. K., Casteel, N., and Weiner, L. P. (1986). In vivo effects of coronavirus-specific T cell clones: DTH inducer cells prevent a lethal infection but do not inhibit virus replication. *J. Immunol.* **136,** 3052–3056.

Stohlman, S. A., Bergmann, C. C., van der Veen, R. C., and Hinton, D. R. (1995). Mouse hepatitis virus-specific cytotoxic T lymphocytes protect from lethal infection without eliminating virus from the central nervous system. *J. Virol.* **69,** 684–694.

Stohlman, S. A., Bergmann, C. C., Lin, M. T., Cua, D. J., and Hinton, D. R. (1998). CTL effector function within the central nervous system requires CD4+ T cells. *J. Immunol.* **160,** 2896–2904.

Sturman, L. S., and Holmes, K. V. (1981). The molecular biology of coronaviruses. *Adv. Virus Res.* **28,** 35–112.

Sussman, M. A., Shubin, R. A., Kyuwa, S., and Stohlman, S. A. (1989). T-cell-mediated clearance of mouse hepatitis virus strain JHM from the central nervous system. *J. Virol.* **63,** 3051–3056.

Weiner, L. P. (1973). Pathogenesis of demyelination induced by a mouse hepatitis virus (JHM virus). *Arch. Neurol.* **28,** 298–303.

Williamson, J. S. P., and Stohlman, S. A. (1990). Effective clearance of mouse hepatitis virus from the central nervous system requires both $CD4^+$ and $CD8^+$ T cells. *J. Virol.* **64,** 4589–4592.

Williamson, J. S. P., Sykes, K. C., and Stohlman, S. A. (1991). Characterization of brain-infiltrating mononuclear cells during infection with mouse hepatitis virus strain JHM. *J. Neuroimmunol.* **32,** 199–207.

Wodarz, D., and Krakauer, D. C. (2000). Defining CTL-induced pathology: Implications for HIV. *Virology* **274,** 94–104.

Wu, G. F., Dandekar, A. A., Pewe, L., and Perlman, S. (2000). CD4 and CD8 T cells have redundant but not identical roles in virus-induced demyelination. *J. Immunol.* **165,** 2278–2286.

Xue, S., and Perlman, S. (1997). Antigen specificity of CD4+ T cell response in the central nervous system of mice infected with mouse hepatitis virus. *Virology* **238,** 68–78.

Yamaguchi, K., Goto, N., Kyuwa, S., Hayami, M., and Toyoda, Y. (1991). Protection of mice from a lethal coronavirus infection in the central nervous system by adoptive transfer of virus-specific T cell clones. *J. Neuroimmunol.* **32,** 1–9.